APPLICATIONS OF SOFT COMPUTING TECHNIQUES IN STRUCTURAL SYSTEM IDENTIFICATION

L. Dihoru[1], C.A. Taylor[1], A.J. Crewe[1], N. Alexander[1]

[1] *Department of Civil Engineering, University of Bristol, UK,*
Email: Luiza.Dihoru@bristol.ac.uk

ABSTRACT :

The seismic behaviour of masonry structures strengthened with fibre-reinforced polymer (FRP) materials has received very little attention experimentally and theoretically. The non-linear nature of these systems often results in mechanical responses that are difficult to predict via classic analytical methods. A neural network (NN) approach for dynamic system identification is presented here. This method addresses aspects such as system non-linearity, dependence on past loading history and noise contamination. Full-scale seismic tests conducted at Bristol University provided a large dataset of measured and computed dynamic state variables. The NN is capable of predicting the system response under a wide range of seismic inputs and for various user-specified reinforcement ratios. The results indicate that the NN non-parametric approach has an important potential in dynamic system identification.

KEYWORDS: neural network, reinforced masonry, FRP, dynamic system identification

1. INTRODUCTION

Numerous investigators have explored the potential use of FRP on masonry structures in order to improve their capacity and ductility under in-plane or out-of-plane loading (Tikalsky *et al*. 1995, Velasquez-Dimas *et. al.* I 2000, Tumialan *et al.* 2003, Krevaikas and Triantafillou 2005). However, the behaviour under true seismic loading has received very little attention and mostly tests under 'simulated earthquake loading' (large number of cyclic tests) have been reported (Ehsani et al. 1999). Simple analytical methods to assess the out-of-plane behaviour of unreinforced masonry (URM) or FRP-reinforced masonry panels were developed based on the flexural theory present in the building codes(Velasquez-Dimas *et. al*., II, 2000, Hamilton and Dolan, 2001). The general trend has been to adapt the monotonic loading assessment methods for seismic loading as well, but the developed models have not been validated through dynamic experimentation. In general, the previous analytical methods could not provide the sophistication needed to describe the complex non-linear and hysteretic behaviour of a real life FRP reinforced masonry structure. The main shortcoming of any empirical approach is that it is based on human assumptions regarding the form of the relationship between the inputs and the outputs of the system. In general, the analytical assumptions are based on parametric studies that depend on the accuracy of the measured data which is often noise-contaminated, incomplete and incoherent. The difficulty of taking detailed measurements of structural response leads to unreliable approximations of dynamic stiffness and damping. Under these circumstances, the authors believe that the neural network approach is suitable in describing the complex mechanics of an FRP-reinforced structure under seismic loading. The advantage of the NN approach is that there is no need for an a priori assumption about the input-output link. More than that, the neural networks can model systems with large numbers of variables and wide ranging inputs. They are resilient to noise and have proved effective in handling non-linearity and hysteresis in many engineering applications. Neural networks entered the civil engineering field in 1990, when Ghaboussi *et al.* employed them for the first time in constitutive modelling. Many other authors have since taken the same route in modelling (Billings and Chen 1992, Chen *et al*. 1995, Bani-Hani *et al*.1998). A comprehensive review of their use in structural identification was made by Adeli and Jiang in 2006.

2. SEISMIC TESTING OF FRP-REINFORCED MASONRY WALLS

Previous tests conducted at Bristol University by Taylor (1998) showed that the unreinforced masonry (URM) infill panels have a non-linear behaviour under seismic loading and that their mechanical response is highly dependent on structure's boundary conditions. The experimental findings obtained on URM constituted the starting point for a recent programme of testing on masonry walls strengthened with FRP. Full-scale seismic tests were carried out on masonry infill panels (L x l x h = 3 m x 2 m x 0.1 m) with different FRP reinforcement ratios (RR = 0, 0.4, 0.6 and 1). The reinforcement ratio represents the percentage of wall area covered by the composite fabric. All panels were top and bottom supported. The applied seismic input was based on an elastic response spectrum for Soil B according to Eurocode 8. The design response spectrum is presented in Fig.1(left) and the matching shaking table displacement time history for an amplification factor (AF) of 65 % is given in Fig.1(right). Amplification factors (AF) ranging from 0 to 130 % were applied to the shaking table displacement time history. Therefore, a wide range of motion inputs was employed in testing and a large set of structure response data was collected. The applied ground acceleration, the wall displacement and the wall acceleration at midheight, as well as the support reaction forces were measured during testing.

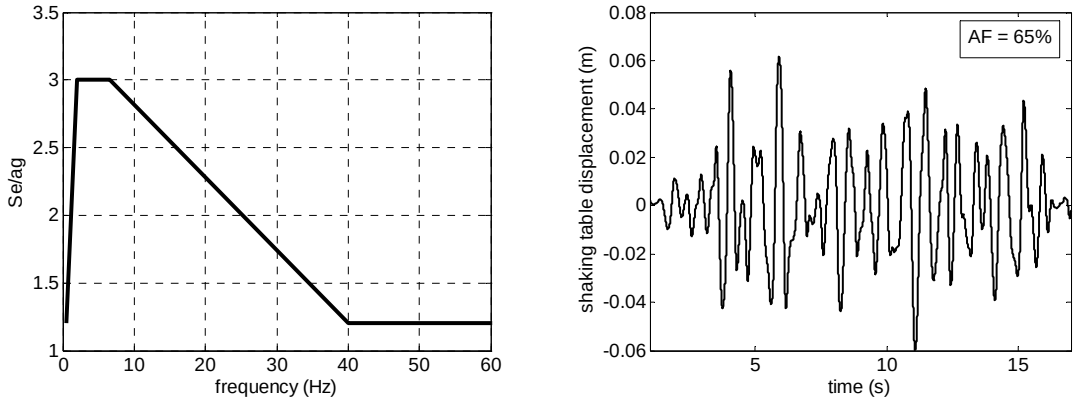

Figure 1 Design response spectrum acc. to Eurocode 8 (left) and matched shaking table displacement time history for AF=65% (right).

The unreinforced masonry behaved elastically in the initial stage of loading and at low seismic inputs (AF less than 60 %). Its arching in vertical plane was almost symmetrical. When the AF reached 65 %, the URM panel developed a horizontal crack at midheight along its entire width and continued arching in the vertical plane. This stage is associated with increasing out-of-plane displacements and crushing of masonry at the contact between the two rotating panel segments. Small translation movements and crushing of the top mortar layer against the panel frame took began to occur. An average quadratic potential well has been fitted for the entire time series in order to understand the pattern of mechanical behaviour. Figure 2 (left) shows how the URM panel's potential well shifts about the origin of motion (AF=90%). The isolated peaks of strain energy are associated with masonry crushing. Figure 2 (right) shows the average potential well fitted for the whole time history of the test SEU1-110 that lead to the URM panel's collapse.

By adding various amounts of reinforcement to the panels, significant changes in mechanical response took place. High reinforcement ratios lead to important increases of panel stiffness and natural frequency of vibration. The FRP reinforced panels behaved like rigid blocks and very small out-of-plane rotation angles were inferred from the displacement measurement. No cracks occurred in the reinforced panels and their behaviour was elastic. The experimental results show that the URM and the FRP-reinforced panels behaved differently under seismic loading. The experimental tests resulted in 64 mechanical response records for four reinforcement ratios. These records were the source of training and testing for the neural network employed in dynamic model identification. The state variables were the panels' displacement and velocity relative to ground, i.e. the shaking table kinematics history was taken into account.

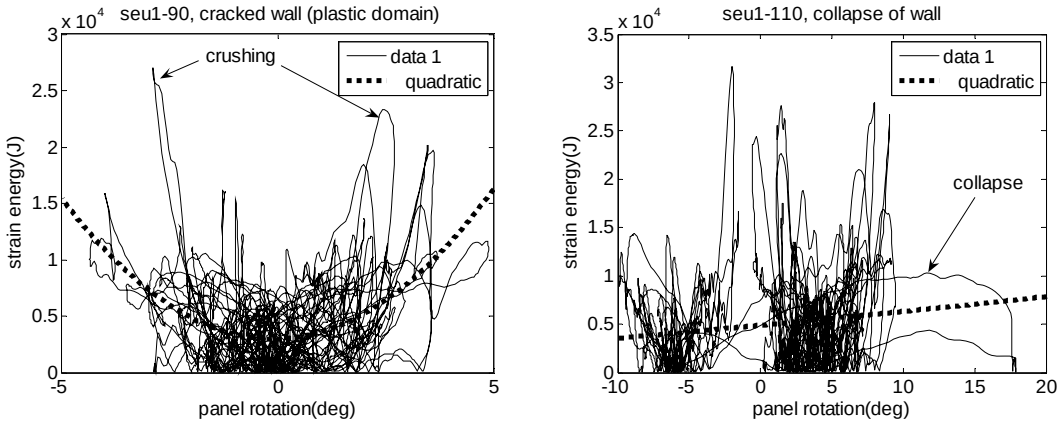

Figure 2 URM panel's average potential well at AF=90% (left) and AF=110% (right) (SEU1).

3. NEURAL NETWORK FOR SYSTEM IDENTIFICATION

3.1. Characterization of dynamic state

If the masonry panel is considered a SDOF (single degree of freedom) system under seismic loading and no other external forces apply to it, then its equation of motion takes the following form:

$$M\ddot{X}(t) + C\dot{X}(t) + KX(t) = M\ddot{G}(t) \tag{3.1}$$

where M, C and K are mass, damping and stiffness matrices, $X(t)$ is the displacement vector and $\ddot{G}$ is the applied ground acceleration. Eqn. 3.1 can be solved in incremental form using, for example, a step-by-step integration method and it poses no problems for linear or non-linear elastic systems. Therefore, when given a set of state variables $X(k)$ and $\dot{X}(k)$ and the dynamic loading $\ddot{G}(k)$, the state variables $X(k+1)$ and $\dot{X}(k+1)$ can be completely determined. However, for non-linear hysteretic systems, the issue becomes more complicated. When representing the evolution of a non-linear dynamic system in phase space diagram, one can see that the position of the system at step $k+1$ is determined not only by its position at step k (Fig.3) but also by its past trajectory.

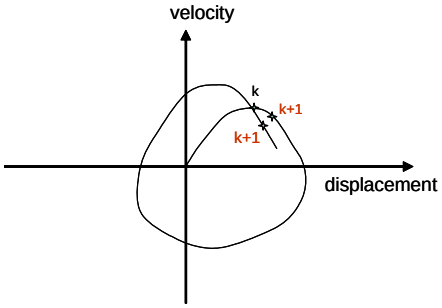

Figure 3 Indeterminacy of dynamic state for a non-linear hysteretic system

From point k, the system could follow different trajectory paths if its past memory is not retained in one way or another. In short, for non-linear hysteretic systems, the state variables $X(k+1)$ and $\dot{X}(k+1)$ depend not only on $X(k)$ and $\dot{X}(k)$ but also on the history of the state variables $X(k-1)$, $X(k-2)$,… $X(k-l)$, respectively $\dot{X}(k-1)$, $\dot{X}(k-2)$ … $\dot{X}(k-l)$, where l is a lag parameter that characterizes the hysteresis in the force-displacement loop. The estimation of l is not a straightforward enterprise in analytical sense. When a neural network is used, the indeterminacy of state variables at step $k+1$ will be associated with noise, unless the past state variables are given as inputs. In general, the more information about the past is

given, the better the neural network will discern between noise and physical data.

3.2. Neural network: architecture and mode of operation

The neural network code was written in Matlab™ (Version 7.1, Neural Network Toolbox). The layout of the NN's mode of operation is given in Fig.4. The network inputs are the wall reinforcement ratio, the ground acceleration time history, the displacement and the velocity at chosen steps in time: $k, k-1, \ldots k-l$. The outputs are the state variables (displacement and velocity) at step $k+1$.

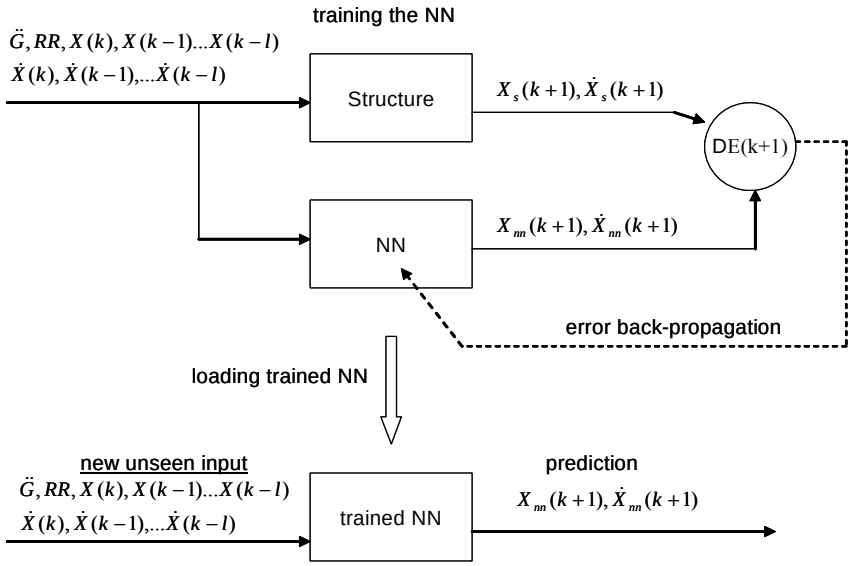

Figure 4 NN for dynamic system identification

The detailed architecture of the NN for 12 inputs (**i**), 2 outputs (**a**), 3 hidden layers of 8 neurons each and 1 output layer is given in Fig.5 below.

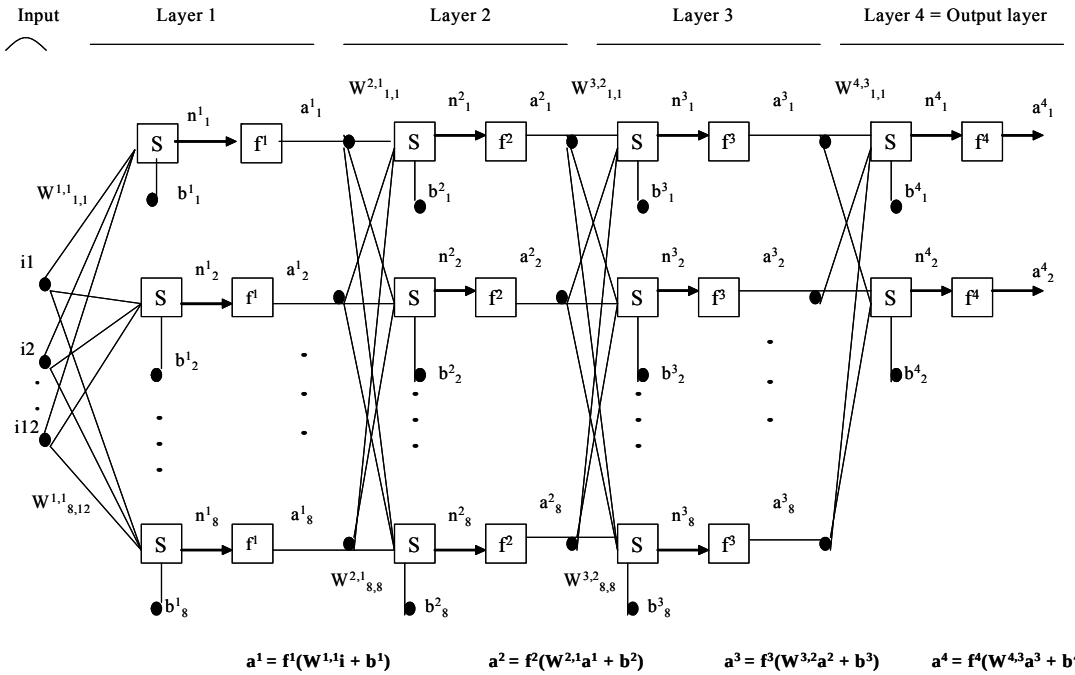

Figure 5 Architecture of the feedforward NN employed (**i:** inputs, **a:** outputs, **f:** transfer function, **W:** weights).

In this example the state variable inputs were $X(k)$, $X(k-10)$, $X(k-100)$, $X(k-1000)$, respectively $\dot{X}(k)$, $\dot{X}(k-10)$, $\dot{X}(k-100)$, $\dot{X}(k-1000)$. According to some authors, three layers of

active units can represent any pattern classification (Beale and Jackson 1990). The neurons are connected by multipliers named 'weights'. They also incorporate 'biases', which are scalars added to the input signal to displace the curve of the neuron's transfer function. The transfer function employed in the internal layers was the 'tansigmoid' function, given by:

$$f(x) = (1 + e^{-\lambda x})^{-1} \tag{3.2}$$

where λ is the gain coefficient employed to control the slope of the transfer function. The 'tansigmoid' function presents the advantage of relating a wide ranging input to a finite output range. Multiple layers of neurons with biases, sigmoid transfer functions, and a linear output layer are capable of approximating any function with a finite number of discontinuities (Demuth and Beale 1990).

The dataset employed in training and prediction is given in Table 1. The training session took place in four stages: assembling the training data, creating the network object, training the network and simulating the NN response to new inputs. The experimental variables (displacement and velocity) employed in training are shown in Fig.6.

Table 1 Datasets for training and testing the NN (AF – amplification factor of seismic input, RR – reinforcement ratio).

NN operation	AF (%)	RR	Test Code	Comments
Training	35	0	SEU1_35	Sampling frequency: 500 Hz
	60	0	SEU1_60	
	110	0.6	SER2_110	
	40	0.4	SER3_40	
	60	0.4	SER3_60	
	80	0.4	SER3_80	
Prediction	110	1	SER1_110	New unseen RR
	100	0	SEU1_100	New unseen AF

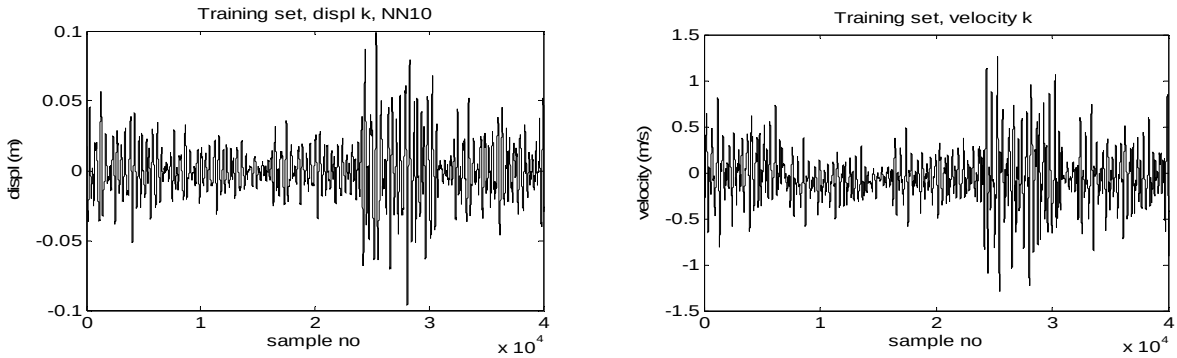

Figure 6 Training set (left: displacement, right: velocity).

The NN uses the default performance function associated with the feedforward networks. The performance function is the mean square error between the outputs of the network and the target outputs from the experimental data set, defined by:

$$E_k = 0.5\Sigma(a_i - t_i)^2 \tag{3.3}$$

where E_k is the global network error after k epochs of training, a_i is the NN prediction of output i and t_i is the target value of output i. The system splits the experimental data randomly in two equal sets: the training set and the test set. The training set is used for learning the pattern connecting the inputs to the outputs, while the test set is used in a post-training analysis (regression analysis) to evaluate the network's performance. The

training pattern consists of an input vector $\left[\ddot{G}, RR, x(k),...x(k-1000), \dot{x}(k),...\dot{x}(k-1000)\right]$ and a desired target vector $\left[x(k+1), \dot{x}(k+1)\right]$. The standard backpropagation with the gradient descent algorithm was used in training: the errors were passed back down the network and the weights between the neurons were adjusted in the direction of the negative gradient of the performance function Eqn. 3.3. The literature describing the details of this commonly-used learning algorithm is very extensive (see for example Demuth and Beale 1990 and Veelenturf 1995). At the beginning of training, the weights and biases are initialized with random values. Then the set of training inputs is shown to the network. During each training iteration (epoch), the network uses its own transfer functions to approximate the relationship between the given inputs and the target outputs. At the end of each epoch the error between the NN outputs and the target outputs times the learning rate is used to adjust the weights of the network. The learning rate is a multiplier with values between 0 and 1, which determines the rate at which the NN converges towards a stable solution.

$$w^{[l]}_{mn}{}^{[p]} = w^{[l]}_{mn}{}^{[p-1]} - \eta\, g^{[l]}_{mn} \quad (3.4)$$

$$g^{[l]}_{mn} = \partial E_p / \partial\, w^{[l]}_{mn}{}^{[p-1]} \quad (3.5)$$

where $\mathbf{w^{[l]}_{mn}{}^{[p]}}$ is the weight connecting neuron no. **m** from **(l-1)**th layer to neuron no. **n** from **l**th layer at the end of epoch no**. p**, $\mathbf{g^{[l]}_{mn}}$ is the current gradient of the error surface, η is the learning rate and $\mathbf{E_p}$ is the global error between the NN output and the target output after **p** learning sessions. The algorithm of gradient descent was implemented in batch mode, i.e. all the inputs were applied to the network before the weights were updated.

3.3. Predictions and performance of the neural network

The trained NN was saved in order to be employed in future predictions. Two new sets of inputs were selected in order to test the prediction capability of the NN: one set which involved a new unseen reinforcement ratio (RR=1, test: SER1-110) and one set which included a new unseen seismic amplification factor (AF=100, test: SEU1-100). The NN prediction for displacement and velocity for the unseen RR=1 is given in Fig.7 and Fig.8, respectively.

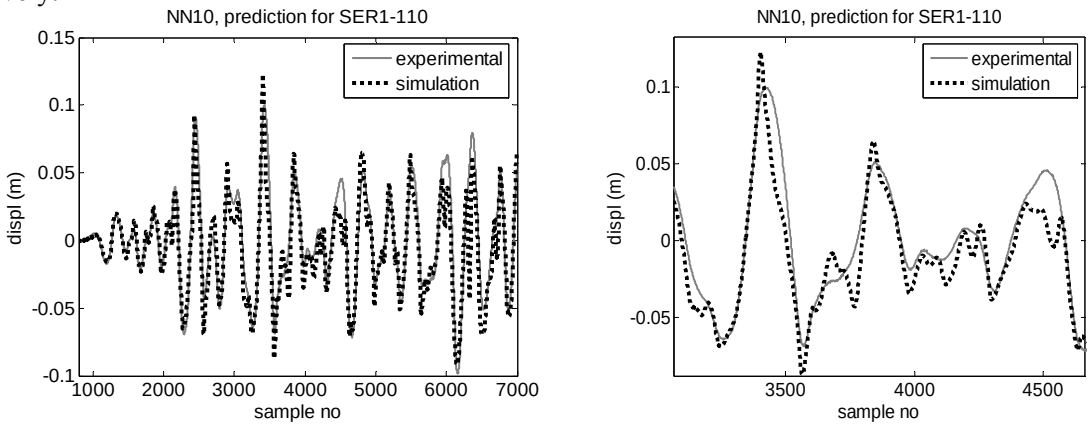

Figure 7 NN prediction of displacement for unseen new input: SER1-110 (RR=1, AF=110, right-detail)

In order to estimate the strength of the linear relation between the predicted and the test state variables, a simple linear regression analysis was performed. The correlation coefficient R was calculated as follows:

$$R = \frac{\mathrm{cov}(A,T)}{\sigma_A \sigma_T} \quad (3.6)$$

where $\mathrm{cov}(A,T)$ is the covariance between the NN simulation (A) and the test set (T), and σ_A, σ_T is the standard deviation of A and T datasets, respectively. Results of the regression analysis are given in Fig.9 for new unseen RR and in Fig.10 for new unseen AF.

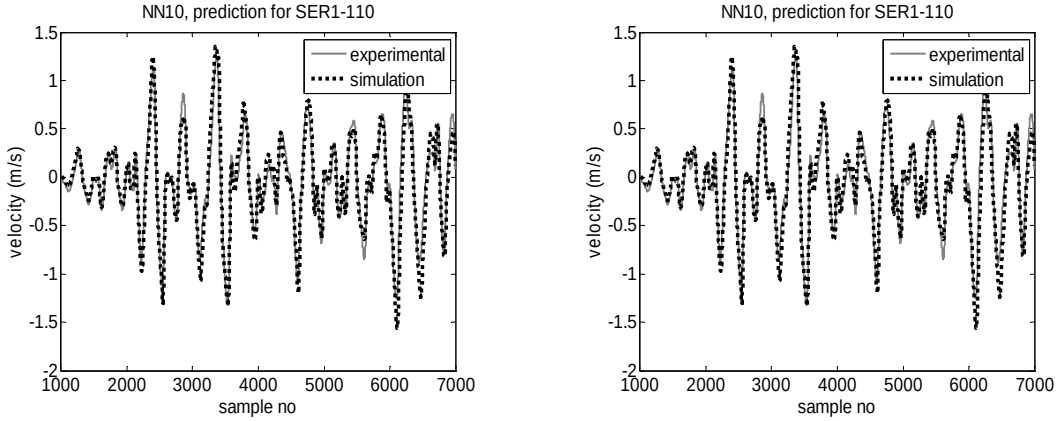

Figure 8 NN prediction of velocity for new unseen input: SER1-110 (RR=1, AF=110, 20000 epochs, right -detail).

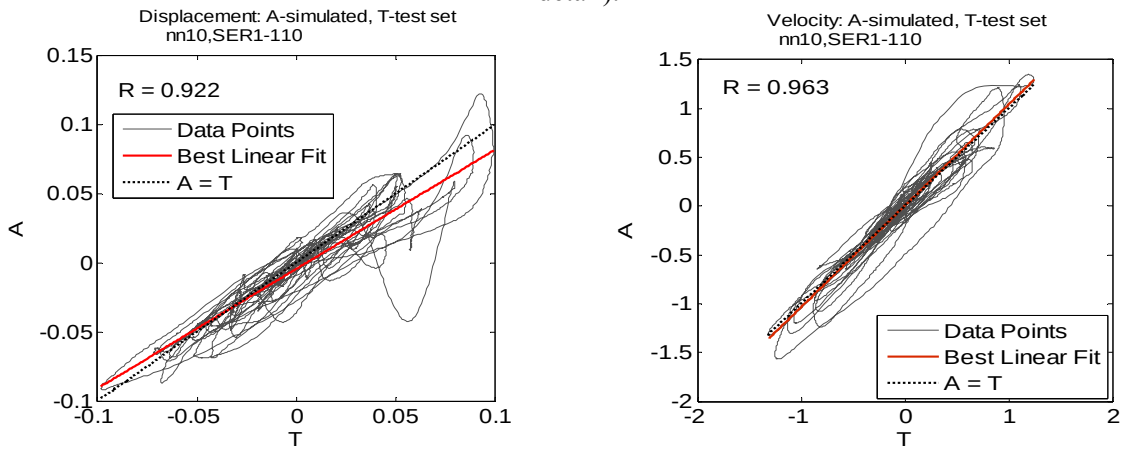

Figure 9 Regression analysis between NN prediction (A) and test set (T) for unseen input: RR=1, AF=110 (20000 epochs. R – correlation coefficient)

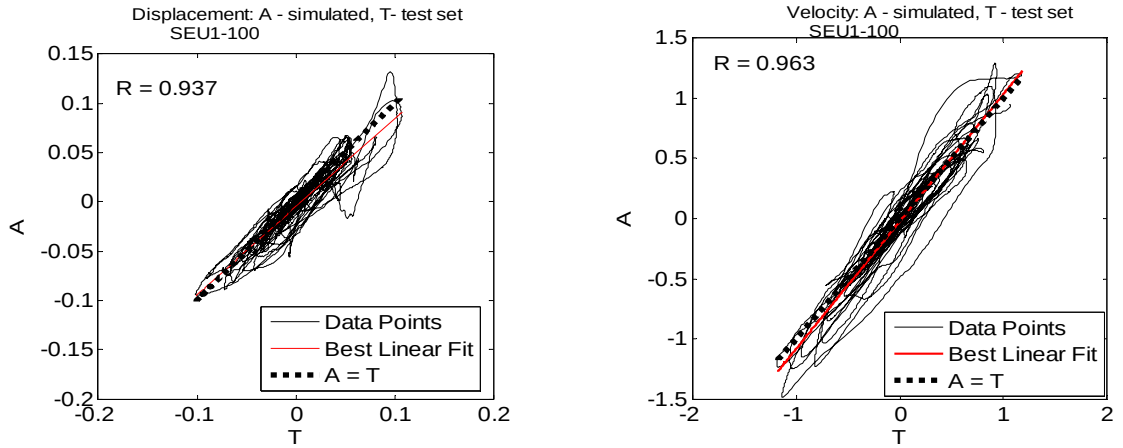

Figure 10 Regression analysis between NN prediction (A) and test set (T) for unseen input: RR=0, AF=100 (20000 epochs. R – regression coefficient)

The learning rate and the number of training iterations are, in general, problem dependent. A larger and noisier data set would require a smaller learning rate and a larger number of epochs of training. The number of training iterations employed in this research varied between 10000 and 100000. It was found that most NNs reached a stable solution after 20000 epochs of training. Theoretically, if the rate at which the weights are adjusted (η) is progressively decreased during training, then the network will be able to avoid the danger of overshooting while moving its outputs closer to targets.

4. CONCLUSIONS

The present work demonstrates that the NN technique is a viable method for dynamic system identification. The neural network could incorporate enough knowledge about the dynamic evolution of stiffness and damping, in order to predict the dynamic state of the system when new unseen inputs (RR and/or AF) were employed. Since the NN training involved both data of elastic and of plastic response, the prediction proved satisfactory for both URM (see SEU1-100 cracked panel) and the FRP-reinforced panel (see SER1-110, intact panel). The datasets for training can be expanded for a wider range of seismic inputs and reinforcement conditions. In principle, the larger and more complex the training set is, the better is the NN in predicting outputs for unseen inputs. The advantage of any trained network is that it can be saved and used both offline as an instrument of prediction or on-line as a control tool. The present work dealt only with its off-line use, but future research may consider its use in a neuro-controller intended for real life structural systems. This research was part of the LESSLOSS (Risk Mitigation for Earthquakes and Slides) project, funded by the European Union under grant no. GOCE -CT-2003-505488. Their financial support is gratefully appreciated.

REFERENCES

Tikalsky P.J., Atkinson R.H, Hammons M.I. (1995). *Journal of Structural Engineering*, **121:2**, 283-289.
Velasquez-Dimas J.I., Ehsani M.R., Saadatmanesh H. (2000). Out of plane behaviour of brick masonry walls strengthened with fiber composites, *ACI Struct. J.*, **97:5**, 377-387.
Tumialan J.G., Galati N., Nanni A. (2003). Field Assessment of Unreinforced Masonry Walls Strengthened with Fiber Reinforced Polymer Laminates, *Journal of Structural Engineering*, **129:8**, 1047-1056.
Krevaikas T.D. and Triantafillou T.C. (2005). Masonry Confinement with Fiber-Reinforced Polymers, *J. Compos. for Constr*., **9:2**, 128-135.
Triantafillou T.C., Deskovic N., Deuring M. (1992). Strengthening of concrete structures with prestressed FRP sheets, *ACI Struct. J*., **89:3**, 235-244.
Ehsani M.R., Saadatmanesh H, Velasquez-Dimas, J.I. (1999). Behaviour of retrofitted URM walls under simulated earthquake loading, *J. Compos. for Constr*., **3:3**, 134-142.
Velasquez-Dimas J.I., Ehsani M.R., II. (2000). Modelling Out-of-Plane Behaviour of URM Walls Retrofitted with Fiber composites, *J. Compos. for Constr*., **4:4**, 172-18.
Hamilton H.R., Dolan C.W. (2001). Flexural Capacity of Glass FRP Strengthened Concrete Masonry Walls, *J. Compos. for Constr*., **5:3**, 170-178.
Ghaboussi J., Garret J.H., Jr. & Wu, X (1990). Material modelling with neural networks. *Proc. of the Intl' Conference on Numerical Methods in Engineering: Theory and applications, Swansea, UK*, 701-717.
Billings & Chen, Chapter 9: Neural Networks and System Identification, K. Warivic, G.W. Irwin and K.J. Hunts, eds., 181-205.
Chen H.M., Qi G.Z., Yang J.C.S. & Amini F. (1995). Neural Network for Structural Dynamic Model Identification, *Journal of Engineering Mechanics*, **121:12**, 1377-1381.
Bani-Hani K., Ghaboussi J. (1998). Non-linear Structural Control Using Neural Networks, *Journal of Engineering Mechanics*, **124:3**, 319-327.
Adeli H. & Jiang X. (2006). Dynamic Fuzzy Wavelet Neural Network Model for Structural System Identification, *Journal of Structural Engineering*, **132**, 102-111.
Taylor C. (1998). Seismic performance of masonry panels for Nuclear Electric plc, EERC Project Report NE395/RP/6, Bristol, United Kingdom.
Eurocode 8: Design of Structures for Earthquake Resistance, Part 1: General Rules, Seismic Actions and Rules for Buildings, BS EN 1998-1:2004.
Beale R. & Jackson T., (1990), Neural computing: An introduction, Bristol and Philadelphia: Institute of Physics Publishing.
Demuth H. & Beale M. (1990). Neural Network Toolbox User's Guide. MathWorks, Inc. 2003, Physics Publishing.
Veelenturf L.P.J. (1995). Analysis and Applications of Artificial Neural Networks, Prentice Hall Intl(UK) Ltd., 70-76.